EURO:TUN 2017, Innsbruck University, Austria

Influence of building geometry on bending and shear deformations of buildings subject to tunnelling subsidence: numerical modelling

Giorgia Giardina[1,2], Stefan Ritter[2], Matthew J. DeJong[2] and Robert J. Mair[2]

[1] *University of Bath, UK*
[2] *University of Cambridge, UK*

Abstract: Masonry buildings in urban areas can be damaged by differential ground movements caused by underground excavations. Existing procedures for the assessment of building damage due to excavation-induced settlements include the effect of the building on the settlement trough in terms of building stiffness relative to soil stiffness. In these procedures, the relative stiffness is calculated by considering either the bending stiffness or the shear stiffness of the building. In this paper, finite element modelling of buildings subjected to tunnelling-induced settlements is used to determine the relative importance of shear and bending deformations in damage predictions. Computational modelling was first validated by simulating centrifuge tests on 3D printed small scale models of masonry buildings subjected to tunnelling in sand. Using a similar modelling approach, a sensitivity study was then conducted on the governing effect of shear or bending deformations for different amounts of façade openings. Results indicate the need to include both shear and bending deformation in assessment procedures, and provide essential data towards this objective.

1 INTRODUCTION

Urban underground projects typically require the assessment of a large number of surface buildings against the risk of being damaged by excavation-induced ground settlements. For this reason, damage assessment procedures need to guarantee an expeditious and conservative prediction which does not require highly detailed inputs (e.g. [1, 2, 3]).

Available assessment procedures tend to focus on the potential damage caused to the building by either the bending or the shear component of the settlement-induced deformation. The bending or shear focus is attested by the way of measuring the building influence on the excavation-induced settlement profile [4, 3]. The magnitude of this influence is associated to the relative stiffness between the building and the soil, which can be evaluated as a ratio between either the building bending [4, 5, 6] or shear [3] stiffness to the soil stiffness.

This paper aims at providing numerical data to develop a more consistent assessment procedure. It investigates the relative contribution of bending and shear deformation in buildings undergoing tunnelling-induced settlements. A finite element model of masonry buildings

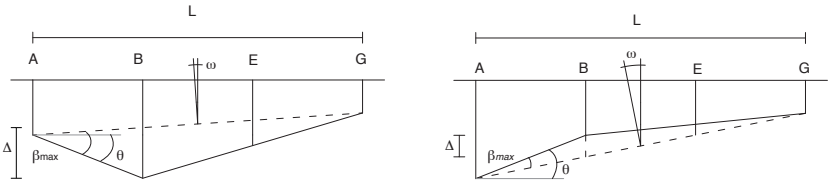

(a) Sagging mode (b) Hogging mode

Figure 1: Deformation parameters: relative deflection Δ, deflection ratio Δ/L, rotation θ, angular distortion (or relative rotation) β and tilt ω.

adjacent to a tunnel excavation in sand is first validated by comparison with the results of centrifuge testing and then used to perform a sensitivity study on the effect of window openings.

2 NUMERICAL MODEL

The numerical models reproduced two centrifuge tests which were performed at the University of Cambridge on 3D printed structures subjected to tunnelling in sand (Fig. 2a). In both experiments, the box containing the soil, tunnel and building model was subjected to an acceleration of 75 g, therefore reproducing the response of a real scale structure 75 times larger. The experimental testing is described in Ritter et al. [7].

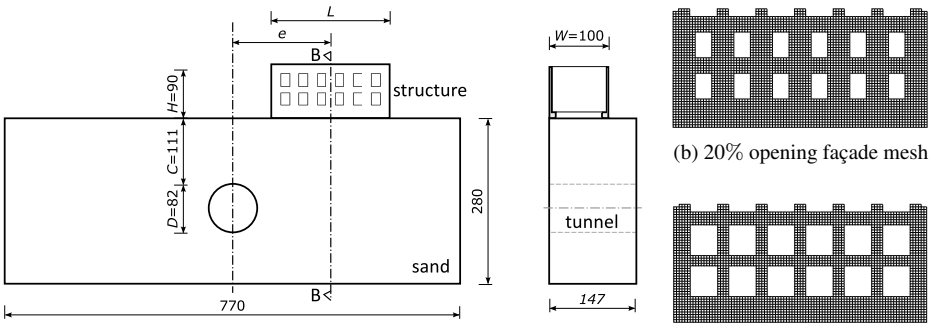

(a) model geometry

(b) 20% opening façade mesh

(c) 40% opening façade mesh

Figure 2: Numerical models reproducing the experimentally tested structures.

In the numerical model, the centrifuge spin-up was simulated by incrementally increasing the gravity acceleration up to 75 g, while the tunnelling-induced settlement profile was obtained by gradually reducing the outward equilibrium radial pressure applied at the tunnel boundary. Both the soil and the building were modelled by quadratic plane strain elements. A nonlinear elastic power low was used to simulate the relationship between the soil strains and stresses; the parameters were calibrated by comparison with the greenfield soil surface displacements measured during the centrifuge spin-up. Giardina et al. [8] reported details and validation of the soil model.

Table 1: Material inputs for the numerical model. See [8] for further details.

Structure	Young's modulus	$E_{\mathrm{w}} = 0.8 \times 10^3\ \mathrm{N/mm^2}$
	Density	$\rho_{\mathrm{w}} = 1.28 \times 10^{-6}\ \mathrm{kg/mm^3}$
	Poisson's ratio	$\nu_{\mathrm{w}} = 0.2$
	Tensile strength	$f_{\mathrm{tw}} = 1.27$
	Ultimate strain	$\varepsilon_{\mathrm{w}} = 0.31\%$
Soil	Ref. Young's modul.	$E_0 = 25\ \mathrm{N/mm^2}$
	Density	$\rho_{\mathrm{m}} = 1.59 \times 10^{-6}\ \mathrm{kg/mm^3}$
	Poisson's ratio	$\nu_{\mathrm{m}} = 0.25$
	Ref. shear modulus	$G_1 = 1\ \mathrm{N/mm^2}$
	Ref. compr. modulus	$K_1 = 2.5\ \mathrm{N/mm^2}$
	Power constant	$n = 0.53$
	Ref. pressure	$p_0 = -1 \times 10^{-3}\ \mathrm{N/mm^2}$
Interface	Normal stiffness	$k_n = 100\ \mathrm{N/mm^3}$
	Tangent stiffness	$k_t = 1\ \mathrm{N/mm^3}$
	Cohesion	$c = 0\ \mathrm{MPa}$
	Friction angle	$\phi = 30^\circ$
	Dilatancy angle	$\psi = 0^\circ$

The building was connected to the soil through line interface elements with zero tensile strength and frictional behaviour (Tab. 1). The latter feature reproduced the transmission of shear stresses due to the rough base interface of the centrifuge models; shear parameters were calibrated by using the tunnelling-induced horizontal displacements of the soil surface observed in the centrifuge model [8].

The building model reproduced a two storey masonry Georgian house on strip foundations; it included two internal transverse walls and windows openings covering 20% (Fig. 2b) and 40% (Fig. 2c) of the total façade area. The plaster-based 3D printed material, used in the centrifuge model to capture potential cracking of masonry, was simulated by a smeared rotating crack model with elastic behaviour in compression and post-cracking linear softening in tension. The material parameters (Tab. 1) were derived by four point bending tests performed on 3D printed material samples [7].

3 DEFORMATION PARAMETERS

This section describes the procedure adopted to separate the bending and shear components of the total tunnelling-induced building deformation. According to Cook [9] the building was divided in three units (Fig. 3a). For each unit the vertical differential displacement was decomposed in tilt, bending and shear deformation (Fig. 3b).

The total deformation was measured as

$$y_{\mathrm{tot}} = \Delta y_A - \Delta y_B \tag{1}$$

with positive downwards vertical displacements.

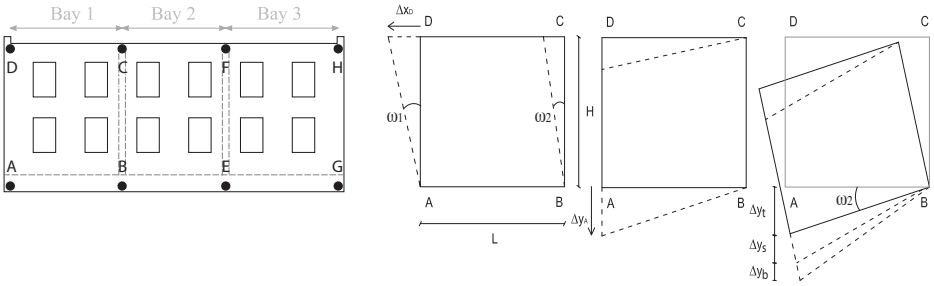

(a) Building bay division (b) Bay 1 deformation parameters (after Son and Cording [3]).

Figure 3: Building reference points and deformation parameters.

The tilt deformation Δy_t is the contribution due to the rigid body rotation. For bay 1:

$$\omega_1 = \text{arctg}\left[(\Delta x_A - \Delta x_D)/H\right] \quad (2) \qquad \omega_2 = \text{arctg}\left[(\Delta x_B - \Delta x_C)/H\right] \quad (3)$$

with ω positive if anticlockwise, and

$$\Delta y_t = \sin(\omega_2) \times L \quad (4)$$

The bending deformation was calculated as

$$\Delta y_b = \text{tg}(\omega_1 - \omega_2) \times L \quad (5)$$

and the contribution due to shear was derived as

$$\Delta y_s = y_{\text{tot}} - \Delta y_t - \Delta y_b \quad (6)$$

4 RESULTS

Figures 4 and 5 compare the experimental and numerical displacements of the models with 20% and 40% of window openings. To improve readability, only the four left points (A B C D) and the four base points (A B E G) are shown for the vertical (Fig. 4) and horizontal (Fig. 5) displacement, respectively.

The soil numerical model has been previously validated against centrifuge testing with no buildings or including simplified surface structures [8]. The good fit to the experimental curves in Figures 4 confirms that the overall model can capture the soil-structure interaction effect on building settlements. The increasing difference between the corresponding base and top point displacements (e.g. Δy_A and Δy_D) indicates the shear and bending deformation of the building portion included between the external right wall and the considered points (e.g. the whole building for Δy_A and Δy_D, bays 2 and 3 for Δy_B and Δy_C).

Figures 5a and 5b indicate a correct simulation also of the horizontal displacement trend, with a consistently larger magnitude with respect to the experimental values. The impact of this difference on the building deformation modelling is limited to the actual discrepancy between the reference point relative displacements; for this reason, the numerical horizontal

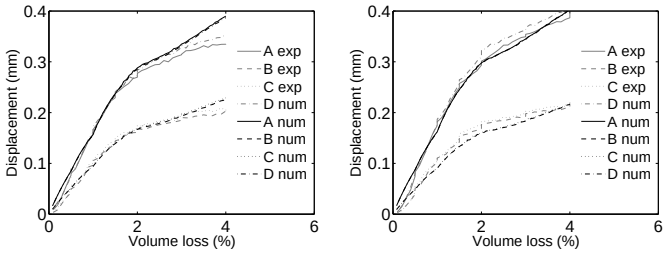

(a) 20% opening (b) 40% opening

Figure 4: Vertical displacements of bay 1 reference points, comparison between experimental and numerical model.

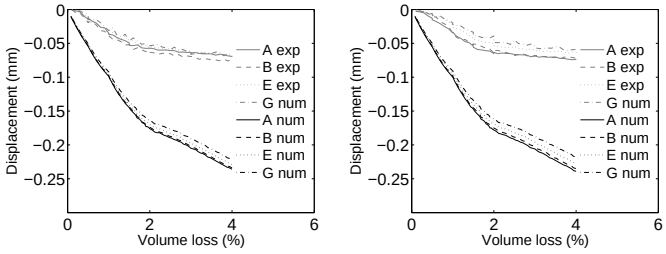

(a) 20% opening (b) 40% opening

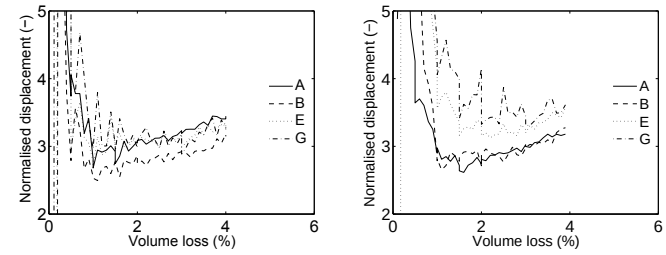

(c) normalised, 20% opening (d) normalised, 40% opening

Figure 5: Horizontal displacements of base reference points, comparison between experimental and numerical model.

displacements are plotted in Figures 5c and 5d as normalised with respect to the experimental values. After an initial adjustment, up to 0.5% of volume loss, the ratio between numerical and experimental values tends to remain constant, suggesting an appropriate modelling of the relative displacement between the reference points.

Following the procedure described in Section 3, Figure 6 reports the relative contribution of shear and bending deformations for each bay of the 20% and 40% window opening models. The trend of increasing deformation with larger volume losses is in line with the experimental observations, as well as the absolute and relative deformation magnitude.

Both the experimental and numerical results show a dominant contribution of the shear com-

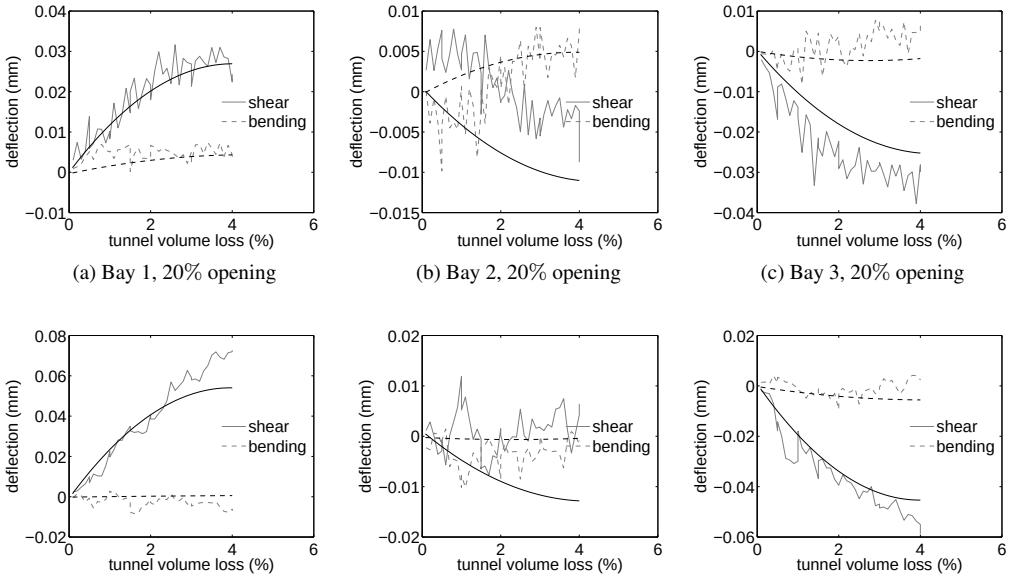

(a) Bay 1, 20% opening (b) Bay 2, 20% opening (c) Bay 3, 20% opening

(d) Bay 1, 40% opening (e) Bay 2, 40% opening (f) Bay 3, 40% opening

Figure 6: Separation of bending and shear components, comparison between experimental and numerical model.

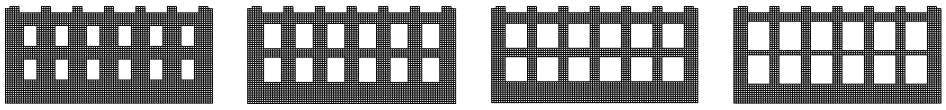

(a) 20% openings (b) 30% openings (c) 40% openings (d) 50% openings

Figure 7: Façade meshes for the parametric study variations.

ponent, which significantly increases for increasing volume losses, while the bending deformation remains generally small. According to the adopted sign convention, negative bending indicates a concave building deflection (i.e. sagging mode, see Fig. 1). A hogging type deformation would be expected for the entire building, due to its position within the tunnelling-induced settlement profile; however, the centrifuge model exhibits a small degree of sagging deflection in the second and third bay, for both the 20% and 40% opening cases. This behaviour is not completely captured by the numerical model, which shows a small sagging deflection only in the third bays. However, the general good agreement between the experimental and numerical deflection contributions enable the use of the numerical model as a reliable tool to investigate different scenarios.

Figure 7 shows the geometrical variations included in a sensitivity study which was performed on the effect of window openings. In the building portion closer to the tunnel centreline (bay 1, Fig. 8a), larger openings lead to a reduced hogging bending deformation, which becomes almost negligible for the extreme case of 50% openings. In the central bay (Fig. 8b), after a similar reduction between 20% and 30% of windows openings, the bending deflection changes in shape and becomes of the sagging type. This behaviour is due to the combination

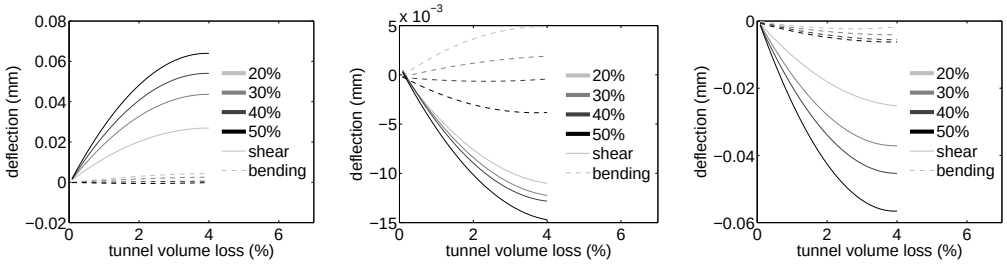

(a) Bay 1 (b) Bay 2 (c) Bay 3

Figure 8: Separation of bending and shear components, variation of opening percentage.

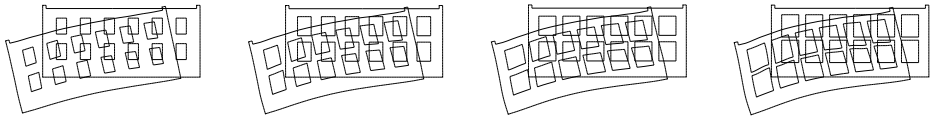

(a) 20% openings (b) 30% openings (c) 40% openings (d) 50% openings

Figure 9: Façade deformed shape for the parametric study variations, magnitude factor=100.

between the higher flexibility of the building with larger openings and the influence of the horizontal component of the tunnelling-induced soil displacements. Figure 9 indicates that this effect is limited to the lower side of the building, and it does not affect the global deformation mode of the façade, which remains predominantly in hogging. In bay 3 (Fig. 8c) the trend is confirmed by an increasing sagging type deformation of the bending deflection. For all bays the shear component keeps increasing with increasing opening percentage, and represents the larger contribution to the total building deflection.

5 CONCLUSIONS

This paper analyses the relative contribution of bending and shear deflection to the tunnelling-induced deformation of surface masonry buildings. Finite element modelling is used to simulate the response of 3D printed models of complex structures adjacent to tunnel excavations, which was modelled in a geotechnical centrifuge. For the first time, numerical results are validated not only by comparison with soil and building displacements, but also by verifying the model capability of reproducing the experimentally observed proportion between bending and shear deformations.

The model is used to evaluate the effect of windows openings on these deformations for a structure located in the hogging portion of the tunnelling-induced settlement profile. The results emphasize the governing contribution of the shear component and indicate the need to reconsider current assessment procedures, which relate the effect of openings solely to a reduction in bending stiffness (e.g. [10]).

6 Acknowledgments

The authors are grateful to EPSRC grant EP/KP018221/1 and Crossrail for providing financial support. The related research data is available at http://dx.doi.org/10.17863/CAM.6492.

References

[1] J B Burland, Standing J R, and Jardine F M. *Building response to tunnelling: case studies from construction of the Jubilee Line Extension, London*. CIRIA Special Publication Series. Thomas Telford, London, 2001.

[2] R J Mair, R N. Taylor, and J B Burland. Prediction of ground movements and assessment of risk of building damage due to bored tunnelling. In R.J. Mair and R.N. Taylor, editors, *Geotechnical Aspects of Underground Construction in Soft Ground. Proceedings of the International Symposium*, pages 713–718, Rotterdam, 1996. Balkema.

[3] M Son and E J Cording. Estimation of building damage due to excavation-induced ground movements. *Journal of Geotechnical and Geoenvironmental Engineering*, 131(2):162–177, 2005.

[4] D M Potts and T I Addenbrooke. A structure's influence on tunnelling-induced ground movements. *Proceedings of the Institution of Civil Engineers: Geotechnical Engineering*, 125(2):109–125, 1997.

[5] J N Franzius, D M Potts, and J B Burland. The response of surface structures to tunnel construction. *Proc Inst Civil Eng: Geotech Eng*, 159(1):3–17, 2006.

[6] K H Goh and R J Mair. The response of buildings to movements induced by deep excavations. *Geotechnical Engineering Journal of the SEAGS and AGSSEA*, 42(3), 2011.

[7] S. Ritter, G. Giardina, M.J. DeJong, and Mair R.J. Centrifuge modelling of building response to tunnel excavation. (Submitted for review to the International Journal of Physical Modelling in Geotechnics).

[8] G. Giardina, M.J. DeJong, and R.J. Mair. Interaction between surface structures and tunnelling in sand: Centrifuge and computational modelling. *Tunnelling and Underground Space Technology*, 50:465–478, 2015.

[9] D Cook. Studies of settlement and crack damage in old and new facades. In *Proc., 3rd Int. Masonry Conf.*, volume 6, pages 203–211, London, 1994.

[10] M Melis and J Rodriguez Ortiz. Consideration of the stiffness of buildings in the estimation of subsidence damage by epb tunnelling in the madrid subway. In *Response of Buildings to Excavation Induced Ground Movements Conference*, London, 2001.